
Initial process of atomic bomb cloud formation and radioactivity distribution

Tetsuji Imanaka

Research Reactor Institute, Kyoto University, Kumatori-cho, Sennan-gun, Osaka, 590-0494 Japan

5

Abstract

In order to provide basic information for the HiSoF project, current knowledge is reviewed about the process of atomic bomb cloud formation and radioactivity distribution. Based on the results of hydrodynamic simulation as well as observations at Nevada test site in US, the time course of the atomic bomb cloud formation was discussed. The amount of radioactivity that could be the origin of local fallout was calculated both for fission products and neutron-induced radioactivity.

From the preliminary analysis using simple assumptions, 0.1 % deposition of fission product radionuclides in the atomic bomb cloud could cause radiation exposure more than 10 mGy, while radiation exposure was at most 1 mGy from the deposition of neutron-induced radionuclides in dust or fire ash after the bombing. More detailed and reliable evaluation is expected through the efforts of HiSoF.

Introduction

The atomic bomb, named Little Boy exploded over the Hiroshima city at 0815 on August 6, 1945. According to the report of radiation dosimetry system DS02 (Young and Kerr 2005), the height of burst (HOB) and the energy yield of explosion are estimated to be 600 ± 20 m and 16 ± 2 kt TNT, respectively. Although official information is not yet available about the detailed structure and composition of Little Boy, the amount of initially loaded uranium is reported to be 64.15 kg, the average ^{235}U enrichment of which is 80 % (Coster-Mullen 2008). Using equivalent values per yield of 1 kt TNT (Glasstone and Dolan 1977), the 16 kt TNT explosion is equivalent to 2.32×10^{24} total fissions, corresponding to a ^{235}U mass of 910 g and a total released energy of 1.6×10^{13} cal. If a spherical ball is made from 64.15 kg of uranium with a density of 19.05 g cm^{-3} , its diameter will be 18 cm, something like the size of a volleyball. The duration of the fission chain reaction that continued in Little Boy is considered to be about 1 μsec .

The most outstanding feature of the atomic bomb explosion is that a huge amount of energy is released within a very short time in a very small space, which produces a core with extremely high temperature ($> 10^7$ °K) and pressure ($> 10^6$ atm). This core expands very rapidly, transmitting its energy to the surrounding materials mainly by low energy X-rays. The entire bomb materials are engulfed and vaporized by the expanding core, which is called the fireball. According to the description in *The Effects of Nuclear Weapons* (Glasstone and Dolan 1977), at

ISBN 978-4-9905935-0-6

Revisit the Hiroshima A-bomb with Database: 1-14

© Tetsuji Imanaka

0.1 msec after a 20 kt explosion, the temperature of the fireball decreases to 300,000 °K with a radius of 40 feet (about 12 m). At this temperature, as the expansion velocity of the fireball decreases compared to the local acoustic velocity, a shock wave appears at the fireball surface and its front moves ahead of the fireball expansion. At this stage, because of the opacity of shock wave heated air, the internal fireball is not visible through the shock wave front. Then, at 0.1 – 0.3 sec after the detonation, as the air becomes less opaque with the temperature decrease, the luminous inner fireball can be seen with a surface temperature of 6,000 – 7,000 °K. The fireball loses its luminosity in several seconds.

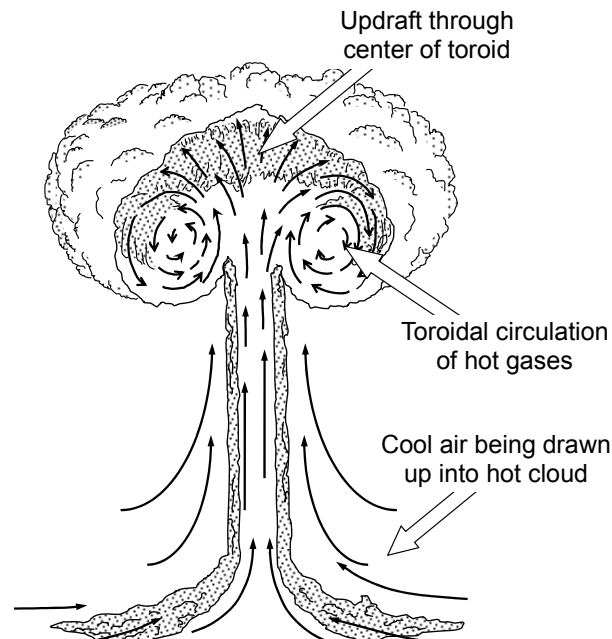


Figure 1 Mushroom cloud formed after nuclear explosion in air at low altitude.

In case of the Hiroshima explosion, the shock wave blast was estimated to arrive at the ground about 1 sec after the detonation, while the fireball began to ascend without touching the ground. As the fireball rose up, a strong upstream of air followed it like a chimney. Then the so-called ‘mushroom cloud’ was formed. A simple conceptual scheme of the mushroom cloud structure is drawn in Figure 1. The formation process and radioactivity distribution of the Hiroshima atomic bomb are discussed in this paper.

Atomic bomb cloud formation

Hydrodynamic simulation for Little Boy explosion

During the processes elaborating DS86/DS02, the US working group carried out hydrodynamic simulation of Little Boy and Fatman (Nagasaki bomb) for the purpose of determining the position of the rising fireball as well as the air density disturbance by the explosion, using the STLAMB code that was developed to simulate hydrodynamic processes for low altitude nuclear explosions. An example of air density contour plot obtained by STLAMB calculation in DS86 is shown in Figure 2 for the Little Boy explosion (height of burst: 580 m, yield: 15 kt) (Roesch 1987). After the initial rapid growth up to a radius of about 260 m, the internal pressure of the fireball reached equilibrium with the ambient air at 0.35 sec after the detonation. At this moment the height of the fireball centre had not yet moved from the HOB at

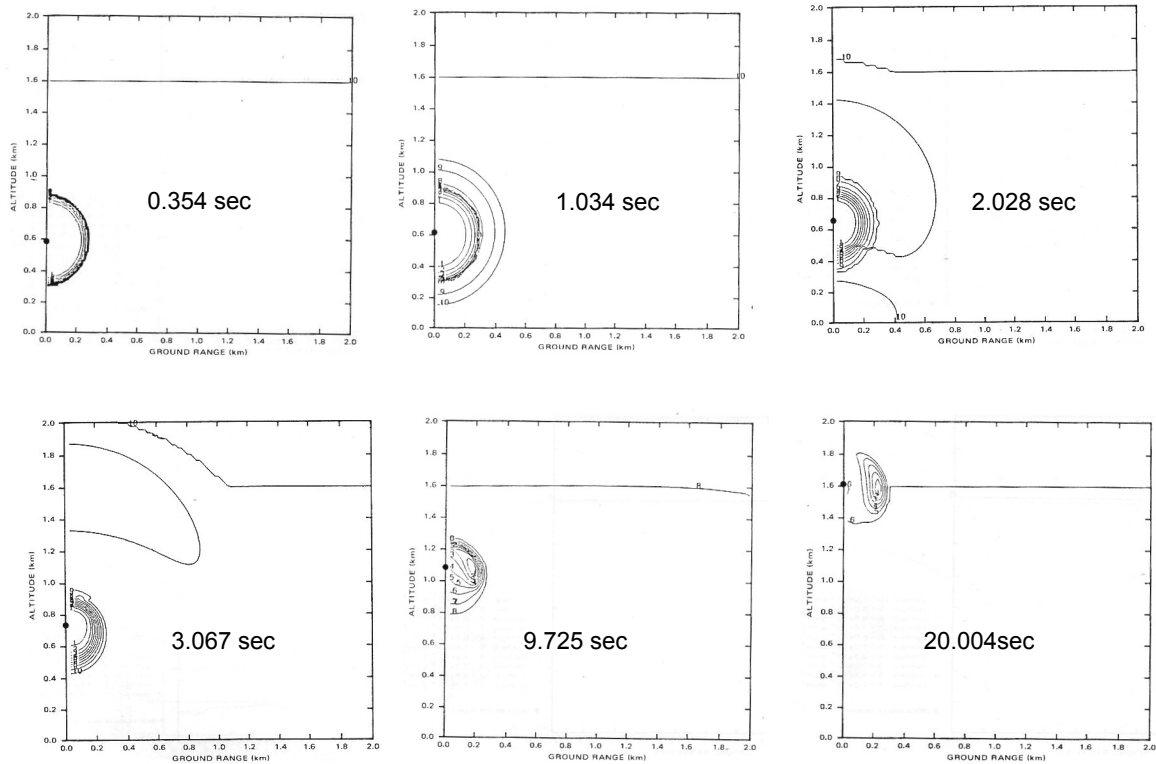


Figure 2 STLAMB simulation of Little Boy explosion in DS86. Air density contour.
 [Reproduced from US-Japan Joint Reassessment of Atomic Bomb Radiation Dosimetry in Hiroshima and Nagasaki, Final Report (DS86), Vols. 1&2, Radiation Effect Research Foundation (1987)]

5

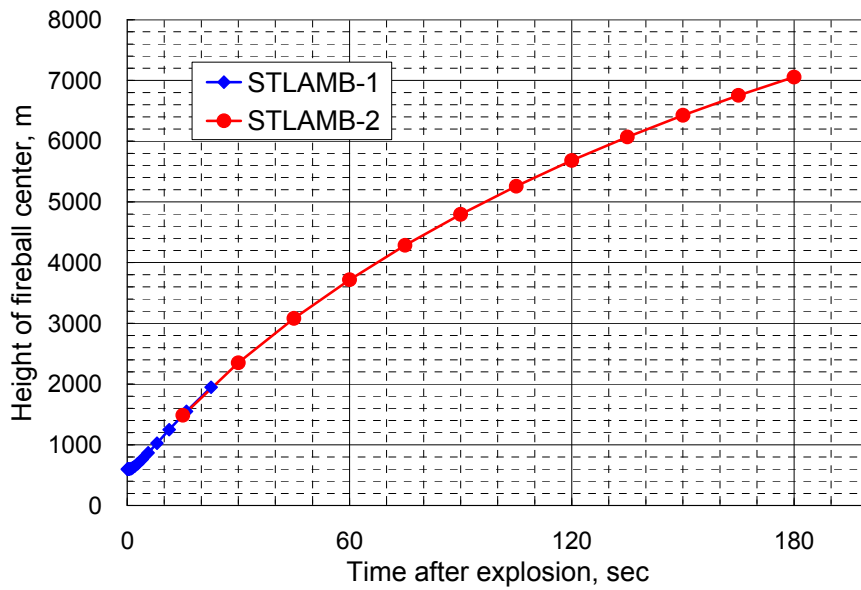


Figure 3 Height of cloud centre after the bombing

580 m. The air density of the fireball centre was $2.26 \times 10^{-5} \text{ g cm}^{-3}$, compared with 1.11×10^{-3} . The shock wave front had already gone ahead of the fireball, (120 m from the fireball surface), but it cannot be seen in Figure 2. At 2.028 sec, the shock wave had been 580 m. The air density of the fireball centre was $2.26 \times 10^{-5} \text{ g cm}^{-3}$, compared with 1.11×10^{-3} already reflected at the ground surface. At 3.067 sec, the reflected wave passed through the fireball. The fireball began rising at a speed of $50\text{-}60 \text{ m sec}^{-1}$. It reached 1100 m at 10 sec, and 1600 m at 20 sec. During this time the shape of the fireball was changing from spherical to toroidal.

Similar STLAMB simulation was carried out during the process developing DS02. The author received the output lists of STLAMB calculation for Little Boy (HOB: 600 m, 16 kt) up to 3 min after the explosion (Egbert 2010). Two sets of STLAMB results were obtained: one

580 m. The air density of the fireball centre was $2.26 \times 10^{-5} \text{ g cm}^{-3}$, compared with 1.11×10^{-3} (STLAMB-1) is up to 30 sec with 18 time intervals and another (STLAMB-2) is up to 3 min with 12 time intervals. From these data, the temporal change of the height of the fireball center is plotted in Figure 3. At 3 min after the explosion, the fireball has risen up to 7,000 m.

15 **Comparison with observation in Nevada test site**

A large report that compiled observation for all atmospheric nuclear tests in the Nevada test site was obtained through the Internet (Hawthorne 1979). From this report, seven tests comparable to the Little Boy explosion were chosen that were conducted by airdrop and exploded at a height where the fireball did not touch the ground. Rising patterns of the atomic bomb cloud for these seven tests were compared in Figure 4 with the STLAMB simulation for Little Boy.

In Figure 4, HOB values for Nevada tests are adjusted to be the same HOB (600 m) as Little Boy. The result of STLAMB simulation is similar to BJ Charlie (14kt) and BJ Dog (21kt) . By extrapolating the tendency of STLAMB simulation to the later period, it can be roughly said 25 “The cloud height of Little Boy was about 8000 m at 4 min, and ascended to about 12000 at 12 min”.

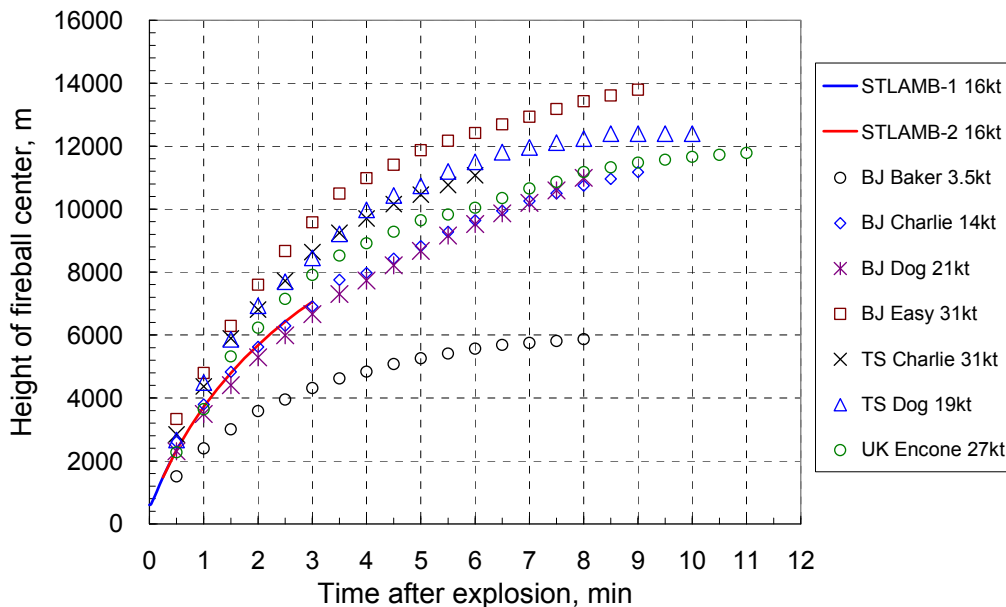


Figure 4 Comparison of cloud ascent data for STLAMB simulation and Nevada observations.

Size of the atomic bomb cloud

Values of the fireball radius obtained by STLAMB simulation are plotted in Figure 5. RFB indicates the horizontal radius of the cloud, while RFBM is considered to be vertical radius of the spheroidal cloud or toroidal cloud. Several observations are also reported for Nevada tests about the cloud size increase. According to these observations, the horizontal diameter increased almost linearly with time up to 20 – 30 min after explosion. The horizontal width (cloud top – cloud bottom), however, seemed to saturate at a constant value after the cloud stopped ascending.

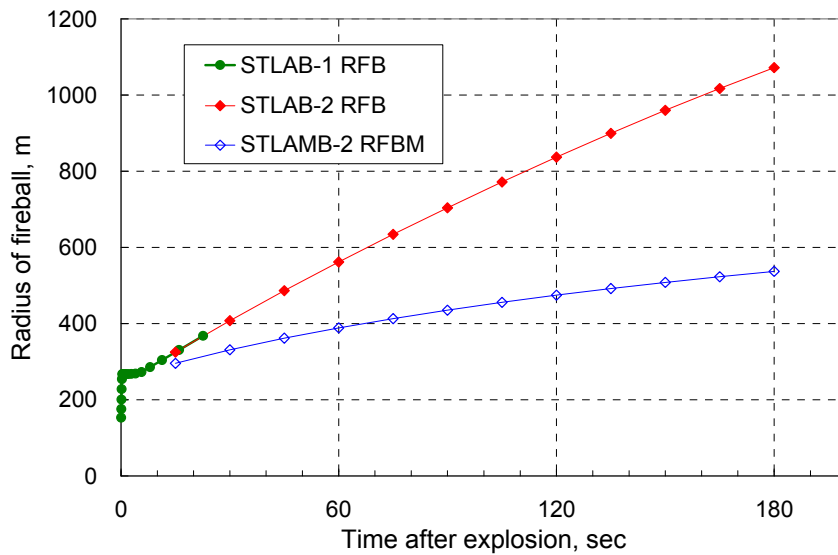


Figure 5 Cloud radius by STLAMB simulation: RFB and RFBM.

10

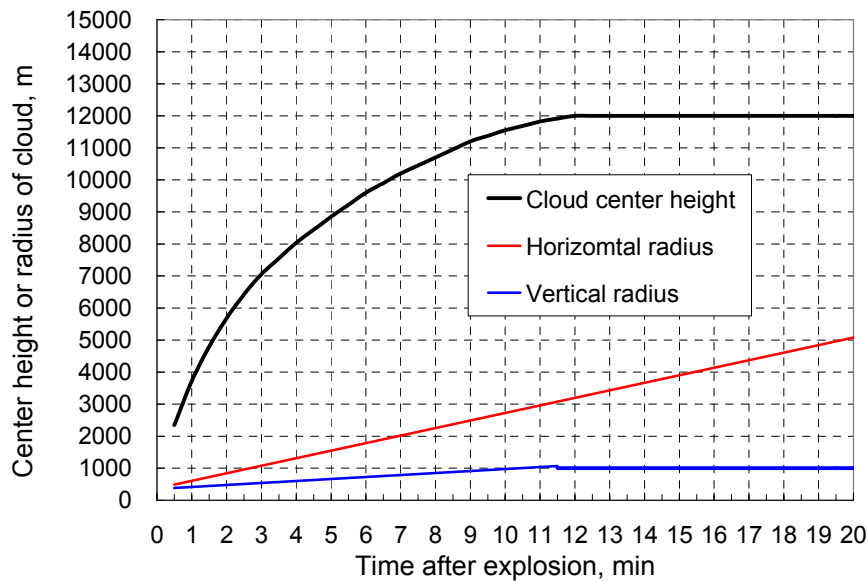


Figure 6 A-bomb cloud formation when there are the same parameters as Little Boy: HOB; 600 m. 16 kt.

Taking into account the results of STLAMB simulation (Figure 5) as well as observations of nuclear tests in Nevada, an ideal case of the atomic bomb cloud formation with the same bomb parameters as Little Boy is plotted in Figure 6 up to 20 min after the explosion. The cloud ascends until 12 min after the explosion and its center height reaches 12 km. The horizontal radius increases linearly with the elapsed time and it becomes 5 km at 20 min, while the vertical radius (half value of the cloud thickness) saturates at 1 km at 12 min.

Temperature decrease and particle formation

As the fireball rises up, its temperature decreases by various mechanisms of thermal radiation, adiabatic expansion and mixing with cool air. With decrease of temperature, vaporized materials of the bomb components begin to condense and solidify, forming small particles that absorb and/or adsorb fission product nuclides. In order to consider the process of particle formation, the time sequence for temperature decrease of the fireball is estimated based on STLAMB simulation as well as literature data.

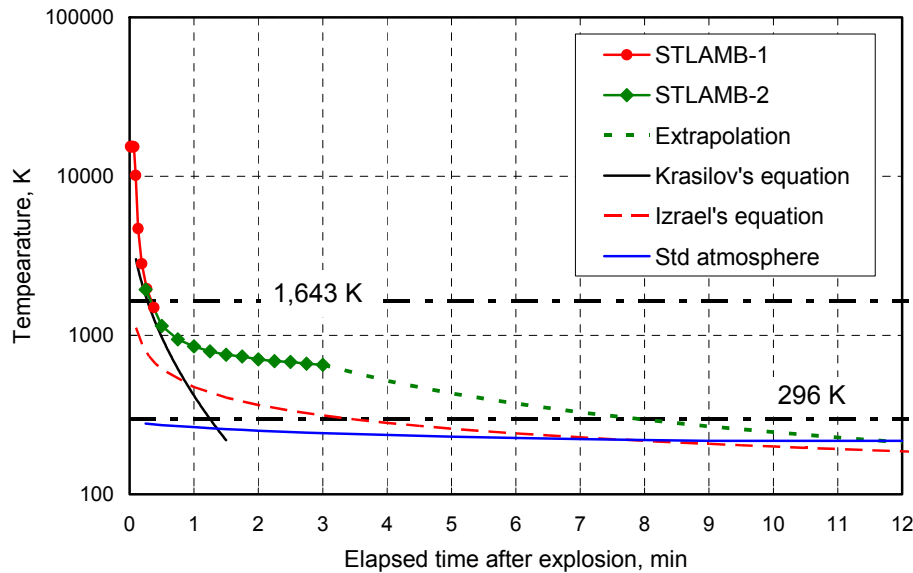


Figure 7 Temperature change of the fireball/atomic bomb cloud.

Although temperature data are not included in the output of the STLAMB simulation, the air density at the fireball centre is provided in the list. Considering that “pressure equilibrium” between the fireball and the ambient atmosphere is attained at 0.4 sec after explosion, the air density can be related to temperature based on the ideal gas equation $PV = nRT$. For example, when compared with $1.16 \times 10^{-3} \text{ g cm}^{-3}$ air density (ambient air of about 300 °K), air density of $2.26 \times 10^{-5} \text{ g cm}^{-3}$ at 1 sec corresponds to 15,400 °K. The temperature decrease obtained by this way from STLAMB calculation is plotted in Figure 7 together with temperature curves proposed from Russian scientists. The black solid line is the equation;

$$T(t) = 7500^\circ\text{K} \exp\left(-\frac{1}{3} \sqrt{\frac{20}{q}} t\right)$$

given by Krasilov (2008), while the red broken line is taken from Izrael’s book (1995); $T(t) = 4000t^{-0.588}$ ($t < 40 \text{ sec}$) or $2183t^{-0.374}$ ($t > 40 \text{ sec}$) for 20 kt air burst. The green dotted line is an

extrapolation of STLAMB-2 up to the point of ambient temperature at 12 min using Izrael's equation of $T(t) = a \cdot t^{-b}$. The blue line indicates ambient air temperature at the height of the fireball (Figure 6). Values of 1,643 and 296 °K are the melting point of iron oxide (FeO) and dew point for air of 27 °C and relative humidity of 80 %, respectively. The STLAMB plot in Figure 7 indicates that droplets of FeO begin to solidify at about 20 sec after the explosion.

Size distribution of particles in the atomic bomb cloud

According to *The Effects of Nuclear Weapons* (Glasstone and Dolan 1977), in the case of air explosion by which no appreciable quantities of surface materials are taken up into the fireball, small particles with a range of 0.01 to 20 μm are formed from condensed residues of the bomb materials. Although it is difficult to say definitely what was the real situation in Hiroshima, the photo taken from the B28 bomber at 2 – 3 min after the bombing (Figure 8) supports the idea that particles of dirt and dust raised by the bomb blast almost remained at low altitude and were not substantially sucked into the fireball or the cap part of mushroom cloud.

The process of particle formation from vaporized materials is discussed in detail by Storebo (1974) dividing the process into nucleation, condensation and coagulation. The size distribution of particles is considered to follow a log-normal law;

$$\frac{dn(r)}{d \ln r} = \frac{1}{\sqrt{2\pi}\sigma} \exp\left(-\frac{(\ln r - \mu)^2}{2\sigma^2}\right)$$

Here, $n(r)$: particle density function for diameter, r ,

μ , σ ; geometric mean and geometric standard deviation, respectively. In Storebo's paper (1974) μ and σ values are evaluated as parameters depending on the initial condition of vapour-to-air mass ratio in the fireball. Assuming that 4 ton of iron was vaporized by the Little Boy explosion

and mixed with the spherical air mass of 260 m radius and $2.26 \times 10^{-5} \text{ g cm}^{-3}$ density, a value of 0.002 was obtained as a vapour-to-air mass ratio. Then, the values of the geometric mean and GSD (geometric standard deviation) were calculated to be 0.2 μm and 1.35, respectively. Histograms of log-normal particle-size distribution are shown in Figure 9 together with the case for a surface explosion for which the particle distribution was arbitrarily chosen as having a geometric mean of 20 μm and GSD of 3.

To consider the possibility of local fallout by gravitational deposition on the ground, the terminal velocity of descending particles is calculated based on Stokes' equation;

$$V_t(D) = \frac{D^2 \rho g}{18\eta}$$

Here, $V_t(D)$; terminal velocity of particle with diameter, D ,
 ρ , g and η are density, gravitational acceleration and viscosity.

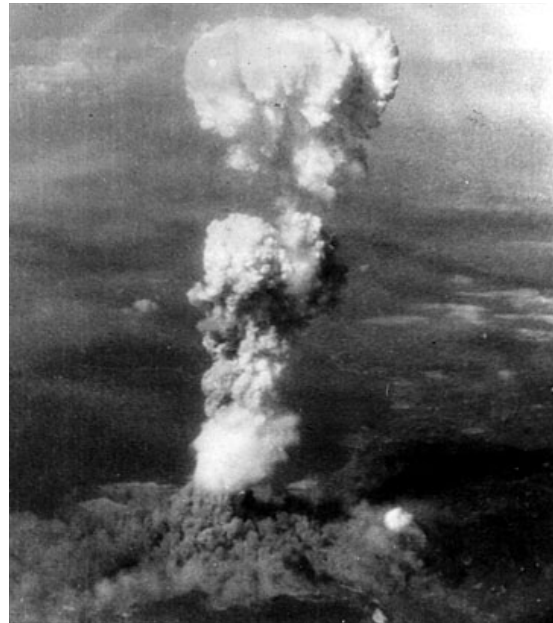


Figure 8 Photo of the Hiroshima bomb cloud taken from the B29, Enola Gay at several min after the bombing.

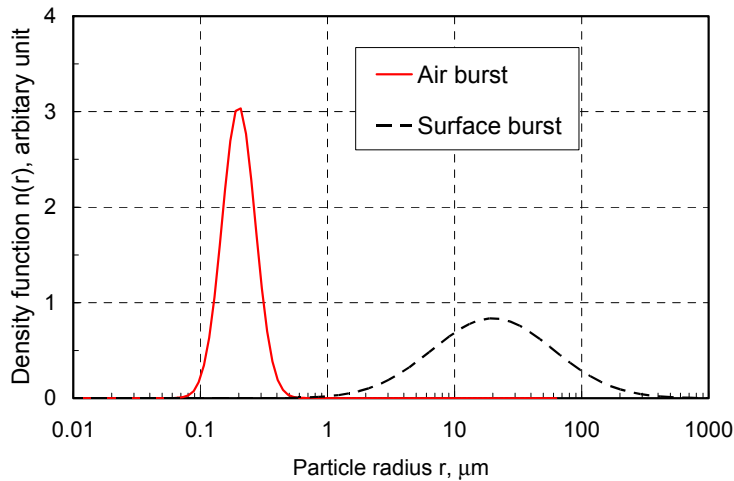


Figure 9 Examples of particle-size distribution for air burst and surface burst. Air burst; mean 0.2 μm and GSD 1.35, Surface burst; mean 20 μm and GSD 3.

The results are shown in Figure 10 as a function of particle radius for three values of particle density. Terminal velocity for particle radius more than 200 μm is not plotted in the figure because deviations from the simple Stokes's equation become significant and velocities are lower in this region than those based on Stokes's equation. As can be seen in Figure 10, deposition velocity drastically changes with particle size. Considering that the fireball created by Little Boy could rise up to about 10,000 m at 10 min after the explosion and the deposition velocity for the supposed particle-size distribution (Air burst in Figure 9) would be less than 0.1 cm s^{-1} , the possibility of local fallout due to gravitational deposition, the so-called 'dry deposition' can be excluded. The only realistic path of local fallout is considered to be deposition on the ground with rainfall, so-called 'wet deposition'. In case, however, particles more than 100 μm were somehow included in the atomic bomb cloud, they could descend to the ground by gravity several hours after the explosion.

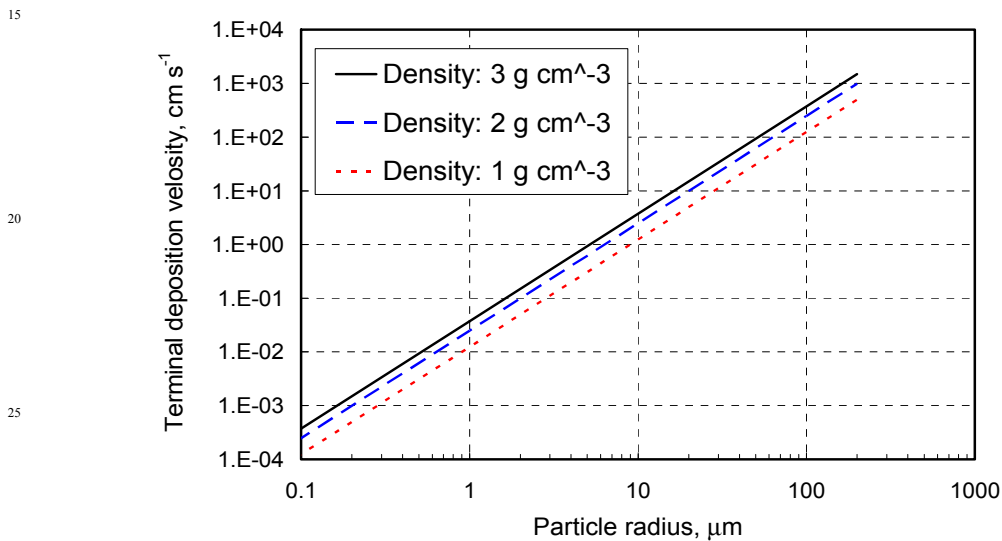


Figure 10 Particle-size dependency of terminal descent velocity for particle density of 1, 2 and 3 g cm^{-3} .

Radioactivity distribution

Local radioactive fallout related with the Hiroshima/Nagasaki bombings are divided into two origins of radioactivity: fission products (FP) from nuclear materials - uranium or plutonium - and neutron-induced radionuclides in exposed materials.

5 *Fission products in the atomic bomb cloud*

The amount of radioactivity of fission product nuclides produced by the 16 kt explosion can be calculated based on physical data such as fission yields, decay modes, branching ratio etc. For the purpose of calculating fission product composition after nuclear fission reaction, a handy program, named FPCOMP.xls was developed using Visual Basic installed in Microsoft
 10 Excel (Imanaka and Kurosawa 2008). Nuclear data for 1,227 FP nuclides ranging from mass number of 66 to 172 were incorporated from the JNDC Nuclear Data Library (Ihara 1989).

The results of the FPCOMP calculation for a 16 kt ^{235}U explosion are shown in Figures 11 and 12. Temporal change of total radioactivity is shown in Figure 11 together with some of individual radionuclide. As can be seen in Figure 11, radionuclides contributing to the total
 15 radioactivity change with elapsed time after explosion, while the amount of total radioactivity steadily decreases along a rather straight line.

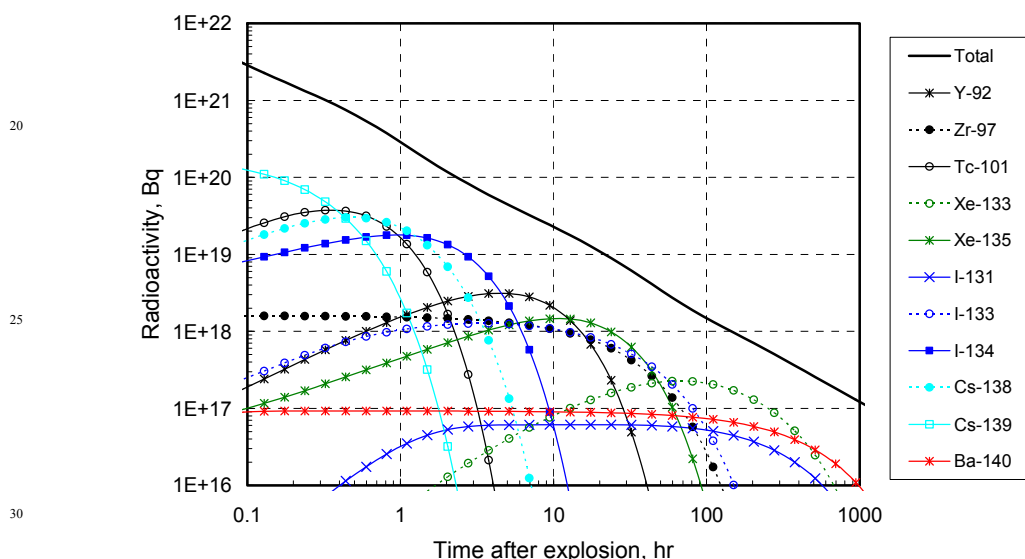


Figure 11 Radioactivity after 16 kt explosion of ^{235}U : Contribution of major radionuclides.

In Figure 12, the total radioactivity is divided into ‘Refractory’, ‘Volatile’ and ‘Rare gas’
 35 according to characteristics of elements that FP radionuclides belong to. The reason for this classification is that the deposition behaviour of FP radionuclides varies a good deal depending on characteristics of the element. Rare gas nuclides do not deposit on the ground. It is known that refractory elements tend to distribute inside FeO particles because they are absorbed when particles are still liquid droplets, while volatile elements tend to be adsorbed on the surface after
 40 solidification of FeO particles. So, particle-size radioactivity distribution can be different depending on the FP radionuclides, which can lead to a different type of deposition on the ground. This phenomenon is called ‘fractionation’ of radioactive fallout (Imanaka et al 2010). The dotted line is the equation of $A(t) = A_0 t^{-1.21}$ that is often used to approximate the decay of total FP radioactivity.

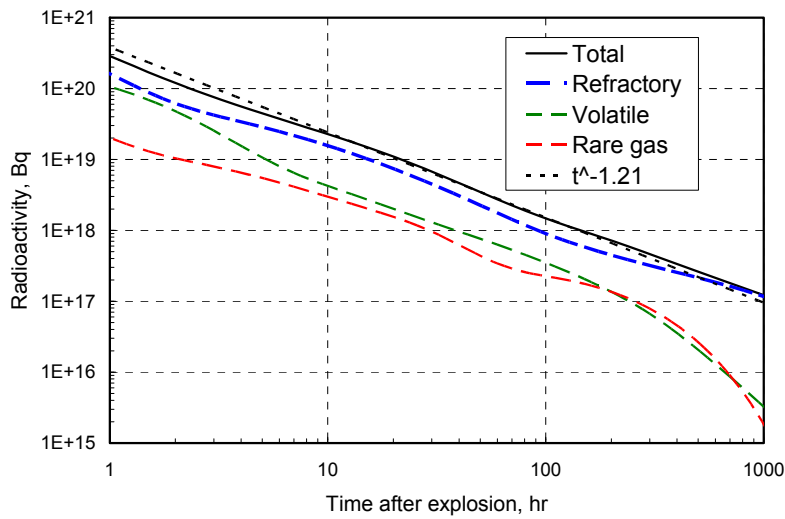


Figure 12 Radioactivity after 16 kt explosion of ^{235}U : Refractory, Volatile and Rare gas.

Radiation exposure from FP fallout

As a sample problem to consider the radiological consequences of local fallout in Hiroshima, radiation exposure rate was evaluated on an assumption that 0.1 % of the total FP radionuclides produced by the explosion uniformly were deposited at 1 hr after the explosion on the area of 66 km² corresponding to the heavy black rain area reported by Uda (1953). For this case the initial deposition density of ^{137}Cs amounted to 1.6 kBq m⁻². Following a retrospective dosimetry method developed by Imanaka et al (2010), 31 nuclides were chosen as representatives of FP radionuclides that could contribute to external gamma-ray exposure when they deposited on the ground. The deposition amount of individual FP nuclides was determined using the theoretical activity ratio to ^{137}Cs . The total density of FP deposition at 1 hr after explosion became 1.2×10^6 kBq m⁻², about 8×10^5 times larger than ^{137}Cs itself. Then, summing up gamma-ray exposure from the 31 FP nuclides, the temporal change of radiation exposure at 1 m above the ground was calculated and shown in Figure 13 for a case without any fractionation effect.

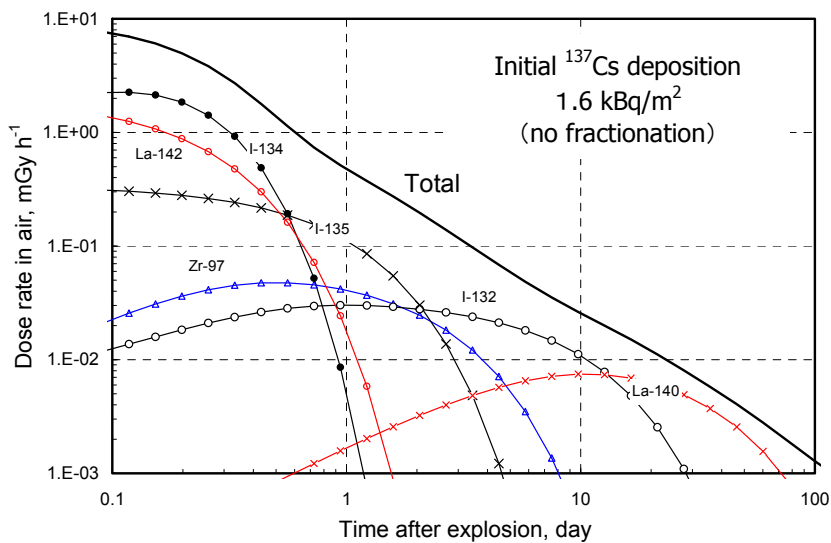


Figure 13 Gamma-ray exposure rate at 1 m above the ground from deposited FP nuclides on the ground.

A radiation exposure rate of 10 mGy h^{-1} was calculated at the time of deposition of 1 hr after explosion. Then, as seen in Figure 13, the exposure rate decreased rapidly with time to 0.6, 0.04 and 0.007 mGy h^{-1} at 1 day, 1 week and 1 month after, respectively. The corresponding cumulative radiation exposure in air was calculated to be 12, 30, 36 and 40 mGy at 1 day, 1 week, 1 month and 1 year, respectively.

Neutron-induced radioactivity in exposed material

At the moment of the explosion, gamma-rays and neutrons are emitted from the atomic bomb as components of the initial radiation. When materials are exposed to neutrons, some elements in them absorb neutrons and become radioactive. This is another origin of residual radiation, called ‘neutron-induced radioactivity’. If significant amounts of dust/soil that contain neutron-induced radioactivity are blown up by the bomb blast in the air, they also can be sources of radioactive fallout.

Through the work to develop DS02 dosimetry system, the neutron energy spectrum released from the Little Boy explosion was calculated at Los Alamos National Laboratory (Young and Kerr 2005). Values of neutron fluence on the ground from Little Boy are given as a function of the distance from the hypocenter (Egbert et al 2007). Based on these data the amount of neutron activation reaction in exposed materials can be calculated (Imanaka et al 2008, Tanaka et al 2008). Manganese-56 (half life: 2.58 h) and sodium-24 (14.96 h) are considered the two main nuclides that can contribute to radiation exposure as neutron-induced radioactivity.

The specific radioactivity of these two nuclides is calculated based on the DS02 fluence values and shown in Figure 14 as a function of distance from the hypocenter. Activation values at 2.5 cm in the ground are about 50 % higher than those at 1 m above the ground. This is because thermal neutron fluence increases with depth of soil to some extent as fast neutrons change to thermal neutrons by losing their energy in the soil layer. The thermal neutron fluence becomes

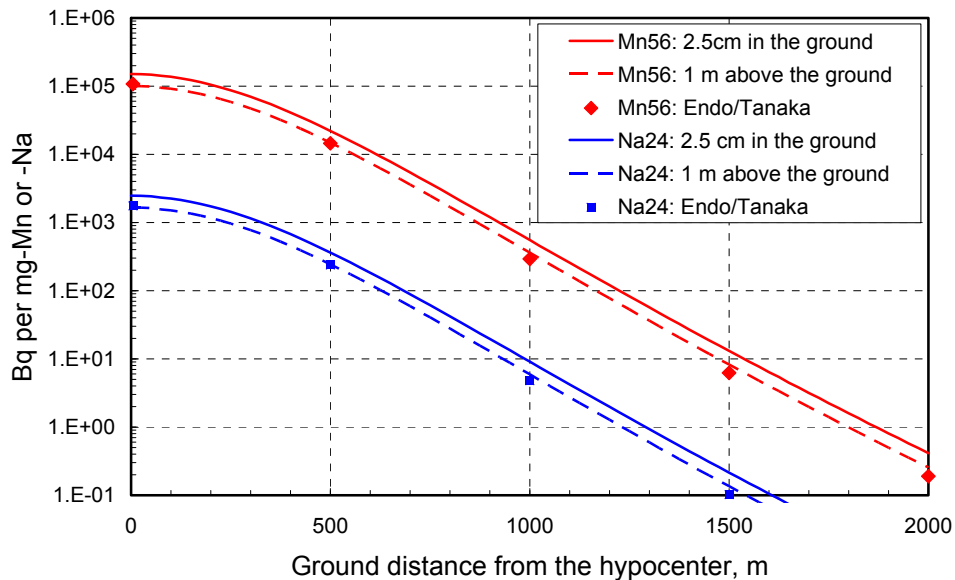


Figure 14 Specific neutron-induced radioactivity for ^{56}Mn and ^{24}Na as a function of distance from the hypocenter. Solid and broken lines are at 2.5 cm in the ground and at 1 m above the ground, respectively, based on DS02 neutron fluence values. Endo/Tanaka data are a result of Monte Carlo transport calculation using neutron leakage spectrum from Little Boy.

maximum around 2.5 cm. As seen in Figure 14, the induced radioactivity decreases rapidly with the distance from the hypocenter. So, here in this article, only activated radionuclides within 500 m from the hypocenter were considered as the origin of local fallout due to neutron-induced radioactivity.

Dust and dirt

According to rough estimation (Aoyama 2011), as a result of the blast damage by the atomic bombing, 1.5×10^4 ton of dust/dirt could be blown up into the air from the 500-m radius area around the hypocenter. The average concentrations of manganese and sodium elements in dust are assumed to be 0.587 and 12.4 mg per g of dust, respectively, based on the Hiroshima soil data in DS86 (Roesch 1987). Using the specific radioactivity data at 2.5 cm in the soil, the total radioactivity contained in the blown-up dust can be calculated to be 5.0×10^{14} and 1.7×10^{14} Bq for ^{56}Mn and ^{24}Na , respectively. If these radionuclides uniformly spread out over the area of 66 km^2 of the strong black rain as given by Uda (1953), the radioactivity densities become 5.8 and 2.5 MBq m^{-2} for ^{56}Mn and ^{24}Na , respectively, at 1 hr after the explosion. Using conversion coefficients of 6.7 and $15 \text{ } \mu\text{Gy h}^{-1}$ per MBq m^{-2} for ^{56}Mn and ^{24}Na , respectively, radiation exposure rate of $76 \text{ } \mu\text{Gy h}^{-1}$ can be obtained at 1 h after the explosion: $39 \text{ } \mu\text{Gy h}^{-1}$ from ^{56}Mn and $37 \text{ } \mu\text{Gy h}^{-1}$ from ^{24}Na . Assuming that these nuclides remain at the same place, a cumulative radiation exposure becomes to be $960 \text{ } \mu\text{Gy}$: $150 \text{ } \mu\text{Gy}$ from ^{56}Mn and $810 \text{ } \mu\text{Gy}$ from ^{24}Na .

Fire smoke and ash

As a result of fire after the bombing, Aoyama estimated about 1.4×10^4 ton of wooden material were burnt out within the 500-m radius area around the hypocenter in Hiroshima (Aoyama 2011). Almost all ash, the weight of which was estimated 1 % of burnt wood, was considered to have risen up into the sky during the fire. Considering the information that pine was the main wood used as house construction at that time in Hiroshima as well as the experimental data on ash composition for various wooden materials (Misra 1993), elemental concentrations in the fire ash are assumed to be 4.04 and 0.06 wt-% for manganese and sodium, respectively. Consequently, using the specific radioactivity data at 1 m above the ground, 2.0×10^{14} Bq of ^{56}Mn and 6.2×10^{11} Bq of ^{24}Na were supposed to be raised up by the fire from the 500-m radius area around the hypocenter if radioactivity converted to values at 1 hr after the explosion.

Using the same method as dust/dirt, radiation exposure rate of $21 \text{ } \mu\text{Gy h}^{-1}$ was obtained at 1 hr after the explosion: 21 and $0.1 \text{ } \mu\text{Gy h}^{-1}$ from ^{56}Mn and ^{24}Na , respectively. The total cumulative exposure was $80 \text{ } \mu\text{Gy}$: 77 and $3 \text{ } \mu\text{Gy}$ from ^{56}Mn and ^{24}Na , respectively.

Conclusions

Main points discussed in this article about the atomic bomb explosion in Hiroshima are summarized as follows:

- The atomic bomb cloud is supposed to have risen up to 12 km at 12 min after the explosion. The radius of the cloud could be about 5 km (Figure 6).
- The temperature of the fireball/A-bomb cloud decreased to 1643 °K, the melting point of FeO at about 20 sec after the explosion (Figure 7).
- Radial size distribution of particles that were formed during cooling process of the fireball and contain fission product nuclides is considered to have a mean less than $1 \text{ } \mu\text{m}$

(Figure 9). Under this condition, the main path of local fallout becomes deposition with rainfall because the possibility of gravitational deposition on the ground can be excluded.

- If 0.1 % of fission product nuclides are assumed to deposit uniformly on the ground of 66 km² corresponding to the strong black rain area, cumulative radiation exposure of 36 mGy is estimated at 1 m above the ground for the period of one month after the deposition.
- As a possibility of local fallout due to neutron-induced radioactivity, very rough estimate for cumulative radiation exposure of 0.96 and 0.08 mGy are obtained due to updraft of dust/dirt by the blast and smoke/ash by the fire, respectively.

This manuscript is prepared to provide basic knowledge about the atomic bomb explosion in Hiroshima, for hypothetical persons who would join HiSoF project as meteorological simulation modellers, but are not familiar with physical process of atomic bomb explosion. The author asks readers to think that all points mentioned in this manuscript are not fixed views of HiSoF, but can be changed flexibly depending on views of person who are going to join our study. The author is ready to provide more detailed information related to the contents of this manuscript when he is asked.

Reference

- Aoyama M., 2011 private communication from Aoyama M.
- Coster-Mullen J. 2008. ATOM BOMBS: The top secret inside story of Little Boy and Fat man. John Coster-Mullen (self-published).
- Egbert S. D. et al., 2007. DS02 fluence spectra for neutrons and gamma rays at Hiroshima and Nagasaki with fluence-to-kerma coefficients and transmission factors for sample measurements. *Radiat Environ Biophys* 46, 311–325
- Glasstone S., Dolan J. P., 1977. The effects of nuclear weapons, Third edition, US Department of Defence and ERDA
- Hawthorne H. A. ed., 1979. Compilation of local fallout data from test detonations 1945-1962 extracted from DASA 1251, Vol.I- Continental U.S. Tests. DNA 1251-1-EX, 1979
- Ihara H. ed., 1989. Tables and Figures from JNDC Nuclear Data Library of fission products, Version 2. JAERI-M 89-204.
- Imanaka et al. 2008. Gamma-ray exposure from neutron-induced radionuclides in soil in Hiroshima and Nagasaki based on DS02 calculations. *Radiat Environ Biophys* 47 pp.331-336.
- Imanaka T., Kurosawa N. 2009. Application and development of FPCOMP.xls for calculating FP composition. Proc. Ninth Workshop on Environmental Radioactivity, Tsukuba, Mar 27-28, 2008, KEK Proc 2008-9 pp51-60 (in Japanese)
- Imanaka et al, 2010. Reconstruction of local fallout composition and gamma-ray exposure in a village contaminated by the first USSR nuclear test in the Semipalatinsk nuclear test site in Kazakhstan. *Radiat Environ Biophys* 49, 673-684.
- Izrael Yu. A., 1996. Radioactive fallout after nuclear explosions and Accidents. Progress-pogoda, St. Petersburg (in Russian).
- Krasilov, 2008. Private communication.
- Misra M. K. et al., 1993. Wood ash composition as a function of furnace temperature. *Biomass and Bioenergy* 4, 103-116.
- Roesch W. C. ad., 1987. Reassessment of atomic bomb radiation dosimetry – Dosimetry System 1986. Vols. 1&2. Radiation Effects Research Foundation, Hiroshima
- Storebo P. B., 1974. Formation of radioactive size distribution in nuclear bomb debris. *Aerosol Science* 5, 557-577.

Tanaka K. et al, 2008. Skin dose from neutron-activated soil for early entrants following the A-bomb detonation in Hiroshima: contribution from β and γ rays. *Radiat Environ Biophys* 47, 323-330.

Uda, M. et al., Kita I. Meteorological conditions related to the atomic bomb explosion in Hiroshima. In: Collection of reports on investigations of the atomic bomb casualties. Science Council of Japan, Tokyo, 1953, 98-136 (in Japanese).

5 Young R. W., Kerr G. D. ed., 2005. Reassessment of the atomic bomb radiation dosimetry for Hiroshima and Nagasaki: Dosimetry System 2002. Radiation Effects Research Foundation, Hiroshima